

# Computer simulation of the phase behavior of a model membrane protein: Annexin V

Martin A. Bates<sup>a)</sup>

*FOM Institute for Atomic and Molecular Physics, Kruislaan 407, 1098 SJ Amsterdam, The Netherlands and Department of Chemistry, University of Southampton, Southampton SO17 1BJ, United Kingdom*

Massimo G. Noro

*FOM Institute for Atomic and Molecular Physics, Kruislaan 407, 1098 SJ Amsterdam, The Netherlands and Physical and Measurement Sciences Group, Unilever Research Port Sunlight, Bebington, Wirral CH63 3JW, United Kingdom*

Daan Frenkel

*FOM Institute for Atomic and Molecular Physics, Kruislaan 407, 1098 SJ Amsterdam, The Netherlands*

(Received 28 November 2001; accepted 31 January 2002)

The bulk thermodynamic properties of membrane proteins originate from a complex combination of molecular interactions. We propose a simple model based on the pair interactions between a model membrane protein, annexin V. The experimental observations of a honeycomb (p6) and a triangular (p3) phase are successfully reproduced with Monte Carlo computer simulations. Grand canonical simulations and a newly developed “strip”-move constant pressure technique reveal the stability of a dilute fluid phase and a dense solid phase, not observed with the current experimental technology. While this model is extremely simple in that it relies only on hard-body and short-range directional interactions, it nevertheless captures the essential physics of the interactions between the protein molecules and reproduces the phase behavior observed in experiments. © 2002 American Institute of Physics. [DOI: 10.1063/1.1463423]

## I. INTRODUCTION

Most of the questions currently being addressed in the field of membrane proteins concern the biological functionality of the protein, and are aimed at correlating the protein structure with biological mechanisms, such as ion transport across the cell bilayer, signal transduction or guest–host recognition patterns. It is known that some proteins express their functionality only when placed in favorable surroundings. For example, ion channels are formed by rings of a dozen trans-membrane proteins that open, under the right conditions, by a concerted action to allow ions to pass along the central barrel.<sup>1</sup> Such synergetic function can only occur if the basic aggregate is formed. More generally, the functionality of some membrane proteins is intricately linked to, and sometimes caused by, the formation of a pattern on the bilayer surface.

The problem of pattern formation in two dimensions has been confronted in several areas of research and various models have been proposed for the study of the aggregation and phase transition in two dimensions.<sup>2</sup> The questions being asked in this context are fundamentally different than those briefly discussed above and concentrate on the prediction of the phase behavior and the pattern formation for more generalized models. In comparison to the models necessary for studies into the biological function of a single molecule or a small group of molecules, these problems require a lower degree of accuracy in the description of the individual mol-

ecules undergoing a phase transition or a self-assembly procedure.<sup>3</sup> Indeed, for computational tractability, simplified coarse-grained potentials are a necessity if we are to study phase transitions in mesoscopic systems. For example, while atomistic models of membrane proteins embedded in a lipid bilayers have been able to evaluate the detailed interaction forces between pairs of protein molecules,<sup>4</sup> this class of model is not useful for mesoscale simulations due to the large computational cost. In contrast, highly simplified models in which the protein is modeled, for example, as a repulsive sphere with a short range attraction, invoking an assumption that the internal structure of the protein is taken to be essentially rigid and nonspecific, are able to predict the changes in the generic phase diagram as the range of attraction is varied.<sup>5</sup> Similarly, pattern formation has been studied when there is a membrane-mediated interaction between anisotropic particles<sup>6</sup> and for nanoparticles self-assembling in strings onto flat surfaces.<sup>7</sup> The use of simplified coarse grained models is, of course, not restricted to two-dimensional (2D) or membrane systems. For example, Carlsson *et al.*<sup>8</sup> have use a simplified model of a sphere with embedded electrostatic potentials to study the self association of lysozyme in water.

In this paper we formulate a coarse-grained model for a membrane adhesive protein, annexin V, which is simple enough to allow us to study systems at the mesoscopic level using Monte Carlo simulations, but contains enough of the details of the interactions between the proteins to reproduce faithfully the experimentally observed phase behavior. This type of model, whilst still crude, goes some way to address-

<sup>a)</sup> Author to whom correspondence should be addressed. Electronic mail: bates@soton.ac.uk

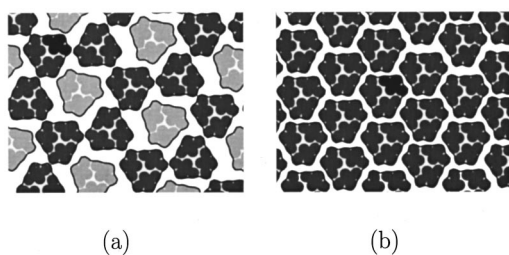


FIG. 1. Schematic electron microscopy maps indicating the structures of (a) the p6 and (b) the p3 phases, after Ref. 10. In each case, the position of a single molecule is shaded black. The trimers are shaded according to the experimental electron density; dark gray represents high electron density and light gray lower electron density.

ing the phase behavior of protein with definite specific interactions as compared to, for example, the isotropic attractive sphere models.<sup>5</sup> The outline of this paper is as follows: In Sec. II, we briefly review the experimentally observed phase behavior of surface adsorbed annexin V. In Sec. III, we devise a simplified model potential which contains the essential physics of the annexin V trimers. Grand canonical simulations using this model are discussed in Sec. IV. The p6 phase is discussed further in Sec. V, where the link between a simple lattice gas model and surface adsorbed annexin V is explored. Other possible, high density regions of the phase diagram are explored with constant pressure simulations in Sec. VI, and the results of all the simulations and theoretical work brought together in a global phase diagram in Sec. VII. Finally, our conclusions are presented in Sec. VIII.

## II. EXPERIMENT

Annexin V is a soluble protein, belonging to the group of proteins that bind to negatively charged phospholipids in the presence of calcium ions in solution. The mechanism of binding involves an extremely rapid first stage in which three proteins cluster together in an almost irreversible manner to form a trimer.<sup>9,10</sup> The strongly bound trimer structure behaves as a single species once it is absorbed onto the surface of the lipid mono or bilayer. The association of the trimer to a planar substrate seems to be sufficient for triggering the self-assembly into 2D crystals and it has long been known that annexin V can crystallize in two crystal forms. These are based on the building block just described, namely the trimer, and show either p3 or p6 symmetry. Experiments on lipid monolayers using electron microscopy (EM) and lipid bilayers using atomic force microscopy (AFM) indicate that the phase with p6 symmetry is the stable phase at low density and that with p3 symmetry at high density.<sup>11,12</sup>

At extremely low surface density, the trimers behave like a two-dimensional (2D) gas, although occasionally one observes small clusters of trimers. The first 2D condensed phase observed on increasing the density exhibits a honeycomb structure (see Fig. 1). The “holes” of this structure tend to be occupied with a relatively mobile trimer, which enjoys a more relaxed interaction with its surrounding cage than a molecule which forms part of the honeycomb lattice, but on average, does have a preferred alignment, indicating that it is not totally free to adopt any position within the

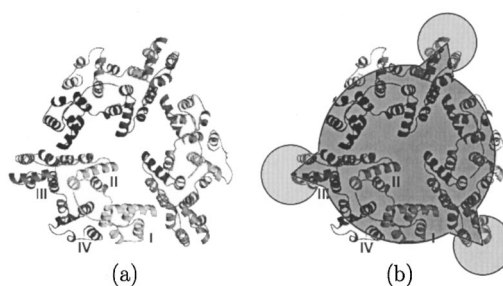


FIG. 2. The simplified model for annexin V: The dark gray regions indicates the hard core of the model and the light gray circles show the location and range of the attractive interactions which occur between segments III in pairs of the real protein.

cage. The corresponding two-dimensional density projection map shows inevitably that the crystals are made of trimers, assembled in “p6 symmetry.” This terminology is not strictly correct since not every cell contains a “captured” trimer and, if it exists, the mobile central trimer does not truly belong to the crystalline network and does not possess the same symmetry as the lattice. This is why the central trimer appears to be less sharply defined density plot obtained from EM.<sup>11,12</sup>

At higher density another crystalline form becomes more stable, where the trimers are packed so tightly that each one is surrounded by neighbors arranged in a (quasi) p3 symmetry class. A schematic indication of the structure of this phase is shown in Fig. 1. The transition to the higher density p3 structure is induced by stressing the p6 system, for example, by transferring the films from an air–water interface to an EM grid, or by increasing the concentration of the lipid ligand in solution.<sup>13</sup> Experiments also suggest that the p6–p3 transition is first order and its reversibility has been monitored using EM and AMF. The first-order transition is characterized by an increase in surface density of trimers of about 15%.<sup>13</sup>

## III. A SIMPLIFIED MODEL

The shape of the trimeric aggregate and a detailed analysis of the crystalline structures suggest the essential features of a simplified model potential. The density map of the p6 phase shows clearly that the trimer–trimer interactions are dominated by (i) repulsive (excluded volume) interactions and (ii) attractive interactions between segments III of neighboring molecules (see Fig. 2 for the labeling of the segments). These segments must be almost perfectly aligned at 180° in order for a transition from the 2D gas to a condensed phase to occur and thus we may speculate that the interaction is highly directional; note that if the interaction was not orientationally specific, then we would not expect to get such a well defined structure. Indeed, the fact that an isotropic 2D liquid is not formed in the experimental system suggests that the anisotropic attraction forces are dominant in causing the pattern formation in the condensed phases. Not surprisingly, the same segment III appears to be responsible for the dominant interaction between the trimers. Here three trimers converge at a cell edge in the p3 phase, at an angle of about 120°. In addition to these observations, molecular mechanics

simulations suggest that segment III is the site at which the dominant attractive interactions occur between trimers.<sup>14</sup> We summarize that the attractive interactions between trimers should be extremely localized, short ranged, and orientation dependent.

These observations lead us to formulate a simplified version of the trimers which is depicted in Fig. 2, based on the following assumptions. The only important particle is the trimer; the monomers in solution play no important role in the 2D pattern formation. The internal structure of the trimer is assumed to be frozen and the trimer may either be strongly bound to the membrane, in which case it interacts with other membrane bound trimers, or it is free in solution and does not interact with the trimers at the surface. We simplify the repulsive core or shape of the trimer by drawing the silhouette as a superposition of an equilateral triangle and a hard disc sharing the same center, with the diameter of the circle the same as the height of the triangle,  $\sigma = h$ . This pair of convex bodies gives a reasonable shape (see Fig. 2) and was chosen over a more complicated single concave body, since overlap tests between these shapes, necessary to simulate the repulsive interactions between the trimers, are both trivial and fast. The vertices of the triangle represent the location of the three segments III in the real trimer. The short ranged, orientation dependent attractions are assumed to exist only between segments III. These attractions are located at the vertices of the triangles, and the strength of these interactions are modelled as a linear ramp increasing from  $-\epsilon$ , for a pair of vertices which are touching, to zero at  $r_c$ , the cut-off distance where the attractions vanish; that is

$$u_1(r_v) = \begin{cases} -\epsilon \left( \frac{r_v - r_c}{r_c} \right) & r_v < r_c \\ 0 & r_v > r_c, \end{cases} \quad (1)$$

in which  $r_v$  is the distance between the vertices of two interacting trimers. As discussed earlier, directionality of the attractive interactions is clearly an important factor, if not the dominant factor, for the formation of the p6 and p3 phases, because it singles out two preferred orientations at  $120^\circ$  (p3 phase) and  $180^\circ$  (p6 phase). The actual functional form of the angular dependence is not important for our model so long as these two angles are preferred, but the EM maps<sup>15</sup> and molecular mechanics calculations<sup>16</sup> suggest that three main qualitative ingredients should be included:

- (1) preferred interaction angles between the III segments at  $120^\circ$  and  $180^\circ$ ;
- (2) comparable interaction energies when two trimers interact at  $180^\circ$  (p6 phase) and three particles interact at  $120^\circ$  (p3 phase); and
- (3) a relative energy penalty for any other angles, especially less than  $90^\circ$ , although we note that angles much less than  $90^\circ$  are disfavored sterically, that is through the repulsive forces.

One possible implementation of the requirements outlined above are summarized in the expression

$$u_2(\theta) = \begin{cases} 1 & \theta < 90^\circ \\ \cos \theta + \frac{1}{2}(1 - \cos 6\theta) & 90^\circ < \theta < 270^\circ \\ 1 & \theta > 270^\circ, \end{cases} \quad (2)$$

where  $\theta$  is the angle between the two vertex vectors; these are defined as the vector joining the center of the particle and the vertex. The total attractive potential with which we choose to model the trimers is just the strength term multiplied by the angular term

$$u(r_v, \theta) = u_1(r_v)u_2(\theta). \quad (3)$$

We should, of course, point out that whilst our particular choice of potential conforms to the qualitative prescription thought to be necessary for the formation of the p3 and p6 phases, we are not simulating “real” annexin V, but rather just a model. Moreover, many models could be devised which all conform to the above prescription; for example, the continuous potential for the angular dependence could be replaced with a piecewise linear potential, the ramp potential for the strength of the interactions could be replaced with a square well and the shape of the hard-body could be taken to be a body with a slight but definitive chirality (ours is clearly achiral). However, the point of these simulations is to understand the highly complicated interaction potential in a more generic way, and so we base our model solely on simplified interactions.

#### IV. GRAND CANONICAL SIMULATIONS

Grand canonical, or constant chemical potential, simulations<sup>17</sup> are particularly attractive for the simulation of the phase behavior of our model since these mimic the conditions under which the experiments are performed. In the experimental system, the protein is either in solution or bound to the membrane as part of a trimer. By varying the concentration of protein in solution, the amount of adsorbed protein, or surface trimer density, can be varied.

The advantage of grand canonical simulations over other common simulation techniques for this model is that one can simulate an open system, in which the number of particles is not fixed. The annexin V system is “open” in the sense that we are interested only in the surface adsorbed proteins, and not in the protein solution. This means that adsorption (or desorption) of a protein trimer onto (from) the surface can be modeled by the addition (or removal) of a model trimer from the simulation. By varying the (surface) chemical potential of the trimers during the simulation, which is equivalent to changing the bulk protein concentration in the real experiments, the surface coverage can be varied.

At low chemical potential, only a few particles are adsorbed on the surface. The adsorbed trimers hardly interact because the probability for a pair of particles to come within the interaction range is quite low and the system shows gas-like behavior. However, if the temperature is low, it is possible to observe the formation of small clusters of trimers, in partially formed hexagonal structures. If the chemical potential is increased past a certain threshold, a large jump in the surface density is observed indicating a first-order transition

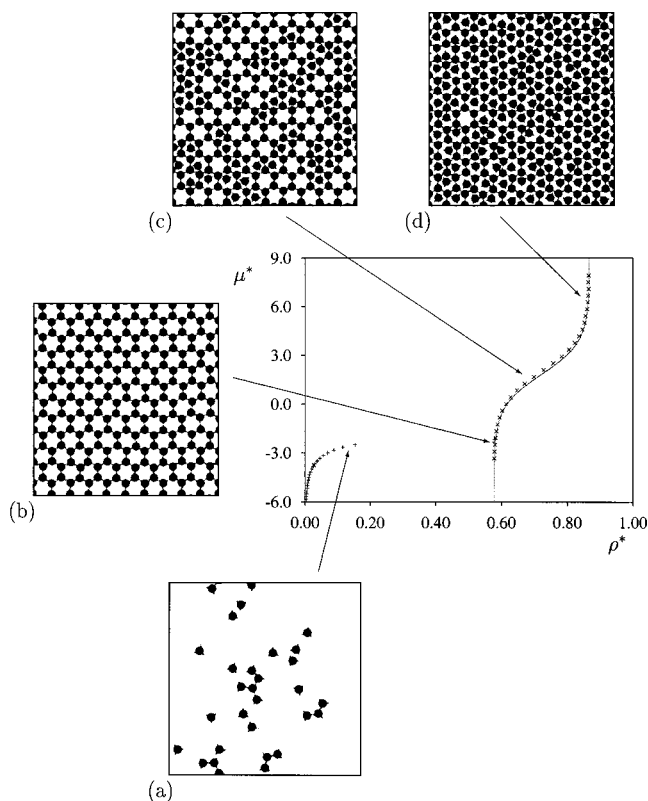


FIG. 3. Equation of state for the annexin V model at  $T^*=0.12$ . Typical configurations are shown in (a) the gas phase and in the p6 phase at (b) low, (c) intermediate, and (d) high surface coverage. Units, temperature  $T^* = kT/\epsilon$ , density  $\rho = N\sigma^3/V$ , chemical potential  $\mu^* = \mu/kT$ .

between the gas and the condensed phase; the equation of state is shown in Fig. 3. A cooperative effect between the adsorbed particles leads to the formation of an open hexagonal structure spanning the entire simulation box, which is clearly identifiable as a p6 phase, as shown in Fig. 3. As the chemical potential is increased further, the density is also found to increase continuously up to a critical value. Similarly, if the chemical potential is decreased, the coverage decreases continuously down to that of the open hexagonal lattice. Example configurations at intermediate and higher surface coverage are also shown in Fig. 3.

The continuous density variation observed in the equation of state corresponds with the filling of the holes in the honeycomb structure; the lattice spacing of the hexagonal lattice is unchanged during this process. Therefore, the surface coverage increases simply by the adsorption of new trimers into the empty cavities. The process is completely reversible, and a lowering of chemical potential causes desorption of the central trimers, leaving the honeycomb network intact. These observations suggest the classification of the trimers into two types; the network or "lattice" trimers and the central or "gas" trimers. The particular geometry of the cages is such that the central trimers experience repulsive interactions when approaching the edges of the cage, and the orientational distribution for the captured trimers is essentially isotropic. Thus in the model, there is no preferred alignment for the trimer trapped within the cage, in contrast to the experimental observation that there is a slight preferential

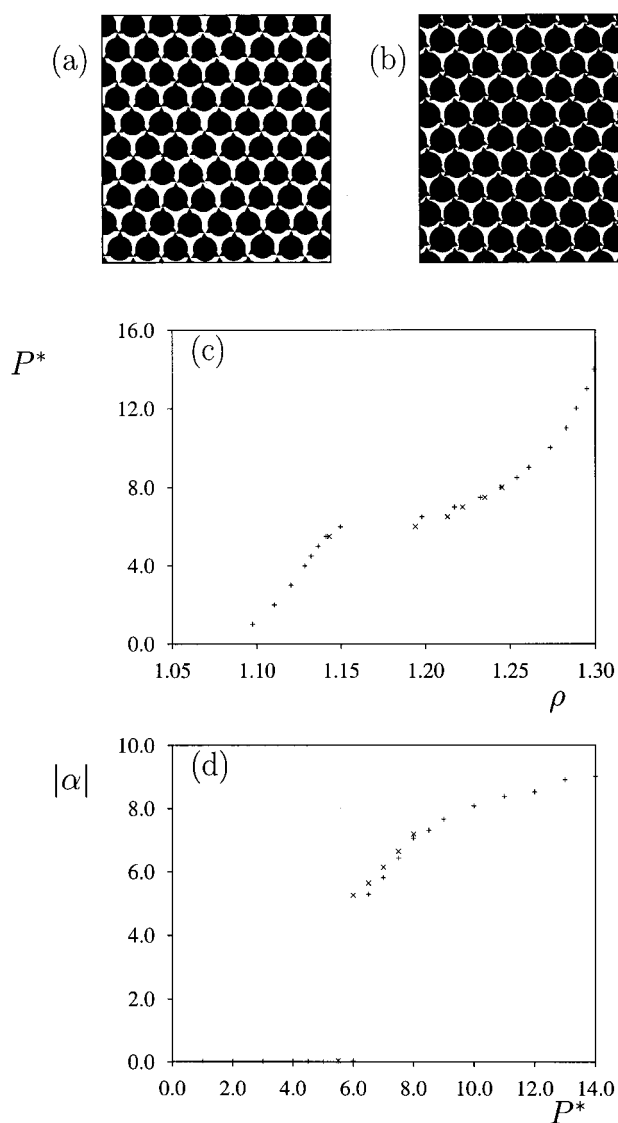


FIG. 4. The two possible conformations of the p3 phase in (a) the "regular" and (b) the "tilted" state. (c) The equation of state obtained from the constant pressure simulations at  $T^*=0.12$ , indicating the first-order nature of the transition between these two states. (d) Tilt angle  $\alpha$ , with respect to the layer normals, again indicating the noncontinuous nature of the transition. (+) compression runs, (×) expansion runs. Units, pressure  $P^* = P/kT$ .

alignment direction, although the smeared out nature of the density map indicates that the central trimer is not strongly held in place. However, it seems likely that if weaker additional attractive interactions were added to the model, such as between segments IV, then the interactions of the captured trimer with the cage would not just be due to the excluded volume and the orientational freedom could be lost. This said, the simple model as it stands clearly reproduces the essential features of the p6 phase behavior.

Once the surface coverage reaches a certain limit, corresponding to all the hexagonal cavities being full, there appears to be no way of adsorbing further trimers onto the surface. However, the simulations indicate that there is a further jump of  $\sim 15\%$  in the density corresponding to a second first-order transition. The new structure, shown in Fig. 4, loses the hexagonal packing in favor of a more com-

pact phase with triangular symmetry, the p3 phase. This phase is also reminiscent of the p3 phase of annexin V (see Fig. 1). The fact that the p3 phase is more stable at higher densities than the p6 phase must clearly be due to the more efficient packing. However, since there is an attractive potential which holds the trimers in particular arrangements, namely at 180° or 120°, this transition is most probably also partly energy driven as well as being entropy driven. Note that, in the model, we choose the energy of a p6-type bond (180°) to be twice that of a p3-type bond (120°). In the *empty* p6 phase each trimer interacts with three others, while in the p3 phase each particle interact with six neighbors in total. The overall potential energy of these two phases is, therefore, the same, at least in perfectly formed, ideal structures. However, since 1/3 of the trimers in the *fully occupied* p6 phase are noninteracting (the “captured” ones), the p3 phase for the model system is also slightly energetically favored at high density. Whilst small modifications in the potential could lower the energy of one phase with respect to the other, this does not seem likely to change the first-order nature of the transition. We summarize this section by stating that the simple model for annexin V is not only able to faithfully reproduce both the p3 and p6 phases, but also predict the relatively strong first-order nature of the transition between them and the associated density change.

## V. LATTICE GAS MODEL FOR THE P6 PHASE

As we discussed in the last section, the trimers assembling into the p6 phase can be ideally divided into two different classes; the lattice trimers which form a rigid hexagonal network, and the gas trimers which can be adsorbed into the cages of the lattice. Of course, while we label the trimers as being of lattice or gas type, in reality the trimers are the same, but are labeled according to their local environment. There is no physical reason that a lattice type trimer cannot become a gas type, and vice versa, although the real kinetics associated with the desorption and absorption of the two species are clearly not available from the Monte Carlo simulations. However, the large energy barrier which must be overcome for the removal of a lattice type trimer is much larger than that for the removal of a gas type trimer, and so it seems likely that the gas type particles are desorbed (and consequently absorbed again) at a much faster rate. Indeed, this is borne out by the fact that in the simulations indicate that the lattice is formed first, presumably due to the strong local attractions between the trimers, and only later are the cages filled. This simulation evidence is further backed up by experimental evidence as lattices can be prepared in a semi-filled state, although no detailed experiments have yet been performed in which the concentration of the protein in solution is carefully lowered to “wash out” the cages to leave a bare lattice.

In this section we show that the p6 gas trimers behave exactly as in an ideal lattice gas model,<sup>18</sup> hence our choice for classifying the trimers as being of gas or lattice type. In the following discussion, we assume that the trimers forming the lattice are assumed to be fixed in position, whilst the gas trimers are free to occupy any empty cell, but do not interact with gas trimers in neighboring cells nor with the lattice

trimers (apart from in an excluded volume way); as we noted above, the assumption that once formed, the lattice is essentially a rigid, nonevolving structure does seem to be entirely valid. Then the only way of changing the density of the system is to either absorb or desorb gas type trimers. Within this simple statistical mechanical model, we can express the chemical potential  $\mu$  of the adsorbing species as a function of the surface coverage fraction  $\theta$

$$\beta\mu = \log \frac{\theta}{(1-\theta)q}, \quad (4)$$

where  $\beta = 1/k_B T$ ,  $q$  is the single particle partition function, and  $\theta = N/M$  is the occupation number, or the ratio between the number of adsorbed gas particles  $N$  and the total number of cells  $M$ . Note that, for our model, the occupation number is not the same as the density, since density involves both lattice and gas type trimers, but it is easy to show that

$$\theta = 2(\sqrt{3}\rho - 1), \quad (5)$$

where  $\rho$  is the density of adsorbed trimers (both lattice and gas type). The single particle partition function  $q$  may be accurately estimated using a free volume argument, assuming that the gas particles are constrained by the hard walls of a single lattice cell, as  $q = \sqrt{3}/16$ . Assuming that the lattice trimers are in fixed sites, which is justifiable since the energy required to deform the lattice is large, the chemical potential (per trimer) of a partially filled p6 phase is given by adding the bond enthalpy per lattice trimer, which amounts to  $-1.5k_B T$ , to the expression for the ideal gas translational entropy contribution. The equation of state for the lattice gas model is compared with the simulation data in Fig. 3. The fact that the data agree with remarkable accuracy, given that there are no adjustable parameters in the theory, indicates that the p6 phase observed for the model appears to be a true physical representation of an ideal lattice gas. We should, however, point out that additional weaker attractive interactions, such as those between segments IV of the trimers, may cause deviation from lattice gas behavior for real systems.

## VI. CONSTANT PRESSURE SIMULATIONS

Constant pressure (or NPT) simulations present a complementary technique to the Grand Canonical simulations,<sup>19</sup> and are especially useful where the particle insertion is inefficient, that is, at high density. However, NPT simulations pose a problem for potentials in which the attractive interactions are very short ranged. Even at low, gaslike densities, the sticky character of the interaction potential enhances the probability of the formation of dimers or small clusters, in which the particles are at specific separations, which cause inefficient sampling of the volume for the following reason. In traditional compression–expansion trials, a new volume is chosen and all the interparticle positions are rescaled, such that the location of the particles in the new box are the same as in the old box, but the separations are scaled. If the particles are well separated, such as in a low density fluid of hard spheres in 3D or hard discs in 2D, compression moves are reasonably efficient. Relatively large volume changes can be made, and still the particles in the

rescaled box do not overlap; expansion moves, of course, cannot lead to overlaps for hard bodies. However, just one dimer or small cluster in a system with a narrow attractive range can drastically affect the acceptance of such a trial move. This is because the particles in the dimer are “bound” to each other over a very narrow separation range, which severely limits the amount the box can be squeezed (or expanded) before an overlap between this pair occurs (or the “bonding” energy is lost). One way out of this is to replace these clusters in the scaled box at their original separations, that is, without rescaling the coordinates.<sup>20</sup> This is often used in atomic detailed simulations of molecules with fixed bond lengths, where any change in the length of the bond upon rescaling would mean that the new state would need to be rejected. Here we describe a different method, based on targeting only the low density, cluster-free, regions of the configuration. Instead of rescaling the coordinates of particles within the whole box as a route to changing the density, we propose a volume trial where a region, in the form of a strip of variable width which spans the simulation box in 2D, is added or removed. The idea comes from a scheme devised by Mackie *et al.*<sup>21</sup> in the context of a similar problem encountered in the simulations of lattice polymers,<sup>21</sup> where a whole lattice line (in 2D) or plane (in 3D) is added or removed.

Any proposed volume trial must satisfy detailed balance. If we consider a strip of width  $dx$  chosen randomly from a rectangular box, containing  $N$  particles and having sides of dimensions  $x, y$ , then the probability that this strip contains  $n$  particles is

$$P(n, x) = \binom{N}{n} \left[ \frac{1}{x} \right]^n \left[ \frac{x-dx}{x} \right]^{N-n}. \quad (6)$$

In order to construct a scheme that satisfies detailed balance and samples the correct limiting distribution, the probability of adding a strip of width  $dx$  to a box of side  $x$ , and moving  $n$  particles from elsewhere in the box into this new region, should be equal to the probability for the reverse move of eliminating strip of width  $dx$  from a box of side  $x+dx$  and redistributing the  $n$  particles over the rest of the box. In other words

$$P_B(x)P(x \rightarrow x+dx, n)P_{\text{accept}}^f = P_B(x+dx)P(x+dx, n \rightarrow x)P_{\text{accept}}^r P(n, x+dx), \quad (7)$$

where the superscripts  $f$  and  $r$  refer to the “forward” and “reverse” trial moves and  $P_B(x)$  is the probability that the box has side of dimension  $x$ . As the system is based on hard-body interactions, if an overlap occurs between the redistributed particles, the trial is immediately rejected. Following an argument similar to that of Mackie *et al.*, we obtain

$$\frac{P_{\text{accept}}^f}{P_{\text{accept}}^r} = e^{-\beta p V} \left[ \frac{x+dx}{x} \right]^N. \quad (8)$$

We have described the method for a hard body 2D system, using trials in the  $x$  direction only, but clearly extensions to allow trials in the  $y$  direction for a 2D system and trials in 3D

systems are trivial. Similarly, the extension to particles with continuous but narrow potentials is also straightforward.

During the simulation the “strip” trial is performed along the  $x$  and  $y$  direction randomly, with the center of the strip also chosen at random. The width of the inserted or removed strip can also be chosen to be either fixed or at random. Note that this is an important difference to the lattice case, where only whole lattice lines (or integer multiples of) can be removed or inserted. We tested three methods based on random strip widths, one in which the maximum width of the strip was fixed at  $2\sigma$ , a similar method but with  $0.1\sigma$  and allowing the maximum width to be self-adjusting, such that on average 20% of the trials were accepted. Surprisingly, all three methods appear to be equally efficient at compressing a gas when the pressure is set corresponding to a state point at which the p6 phase is stable. We may expect that the large width strip moves should be more efficient than the small ones; however, the rate at which the density changes (with “Monte Carlo time”) is essentially the same for these methods. Presumably, although the large strip can remove a large volume, these moves are more likely to be rejected since a relatively large number of particles must be redistributed. In contrast, typically no particles need to be redistributed for the narrow strip trial. As the density approaches liquid-like densities (more than about 30% of the close packed density), the self-adjusting route works more efficiently than either. Somewhat surprisingly, the most efficient way to equilibrate the volume at these densities using the strip trial is to use extremely narrow strips ( $\sim 0.01-0.05\sigma$ ). Again, this can be understood in the sense that, on average, no particles need to be redistributed from such a narrow strip and so no overlaps occur. This is also important when the cluster formed percolates from one side to the other, as very narrow strips can still be removed between two or more “bound” particles.

Note the difference between this situation and that with conventional constant pressure trials. For this method, the possibility of rejection is approximately proportional to the probability that a pair of particles are tightly bound in the narrow strip. In contrast, for conventional moves, this is approximately proportional to the probability that a tightly bound pair occurs anywhere in the box. This said, however, the method is not perfect as large gaps may occur when the cluster percolates across both box dimensions, and the simulation will eventually become bottlenecked if the motion of the particles around the edges of the cluster is very slow. In this situation, it is clearly better to start from a number of crystals of predefined structure, with no voids, to obtain the high density branch of the equation of state. Although the compression branch will never match the expansion side of the equation of state due to the voids, jumps in the density in the compression branch at least indicate that a transition has taken place on increasing the pressure.

Simulations were performed using (i) just conventional moves and (ii) both conventional volume trials and strip volume trials, chosen at random. Using the strip method, we find that initial equilibration from a gaslike system at low density to a condensed system is much more efficient than using traditional moves alone. The rate at which the density

changes is between 20 and 50 times faster than using traditional moves alone, although this is clearly temperature dependent. Indeed, at high temperature, clusters should not form and so no equilibration problems would be observed, although we are not so interested in this regime. By increasing the pressure, we have observed the formation of p6 and p3 type clusters, which eventually percolate through the simulation box. However, we should point out that, while the simulations give us an idea of the pressure range over which the phases are stable, they are not a good route to accurate thermodynamic data. This is because, for example, if an empty p6 structure has formed in a system with fixed number of particles, the change from an empty lattice to a full lattice is a very large perturbation. Some of the lattice must be destroyed, such that the lattice still fits in a commensurate way into the simulation box and the particles removed redistributed into the holes. This sort of system is, of course, much more effectively simulated by allowing the number of particles to change, that is, in a grand canonical ensemble, as already described.

The NPT simulations, equipped with the combined strip and traditional volume trials, become useful in the treatment of the high density phases, in which the probability of insertion is extremely low, where grand canonical simulations either fail or are extremely inefficient. Since insertions are essentially forbidden, the strip moves are restricted to ones in which no particles are redistributed. However, we continue to try these types of trials, since removal (or insertion) of narrow particle devoid strips are accepted with slightly higher probability to conventional trials. Constant pressure simulations started in the p6 phase (taken from the grand canonical simulations) are found to undergo the p6–p3 transition at essentially similar densities to those observed in the grand canonical simulations. Thus as the pressure is increased, the p6 phase is not indefinitely stable and we observe a transition to the p3 phase. Somewhat surprisingly, the simulations indicate that there are two stable forms of the p3 phase. Even if the density range over which the p3 phase is stable is rather narrow, we can distinguish between a “straight” p3 and a “tilted” p3\* phase at low temperatures, as shown in Fig. 4, with the former stable at lower densities and the latter at higher densities. In the straight version, the three vertices, representing segment III in the real system, join at a cell corner rigorously at 120°. In contrast, in the tilted version, the three vertices assemble slightly off-center. Hysteresis, and small density jumps, in the equation of state obtained from the NPT simulations suggests that the transition between these two states is first order. As the pressure is increased, the tilted version has to respond by using the available volume more efficiently, and we observe that the tilt angle increases as the density increases, across the (narrow) range of stability of the tilted p3\* phase. The tilt angle is constant in magnitude and sign for all the trimers within the (small) systems we have investigated. Thus the whole system responds to the density increase by tilting in the same direction, even though the model trimers are not chiral themselves. Presumably, a random fluctuation to a chiral-type cluster propagates through the system. Indeed, we have observed the two possible orientations for the tilt angle in dif-

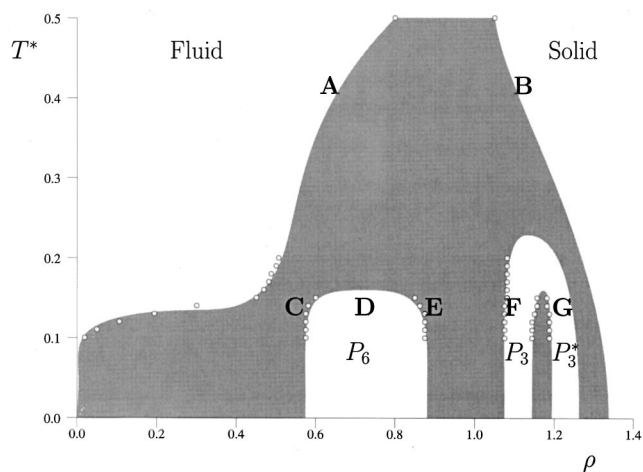


FIG. 5. The generic phase diagram. At low temperatures, the phase sequence is observed to be gas-P6–P3–P3\* (tilted), and presumably ends in the close packed solid phase at extremely high pressures. At high temperatures, only fluid and solid phases are observed. The temperature for which the p6 phase is no longer stable is found to be lower than that for the p3 phase. The p3–p3\* (tilted) transition appears to be continuous at relatively higher temperatures, and a p3–p3\* critical point is present in the phase diagram. The bold letters refer to the various phases observed, as discussed in the text (Sec. VII).

ferent simulation runs, as we expect. However, the addition of even a weak chirality to the particle shape may induce spontaneous chirality to the p3 phase, and indeed a chiral p3 phase may be the only stable p3 phase. At higher temperatures, the p3 to p3\* phase transition appears to be continuous.

At even higher densities attractions become almost unimportant with respect to the enormous pressures applied (especially at high temperature), and the system relaxes using the most efficient packing structure, recurring to close packing. The deviations from the hard-disc close-packed structure are obviously caused by the vertices of the triangles. The particles tend to interdigitate along the lattice rows and show an up–down–up–down pattern, although this does not propagate to long range. At low temperatures (that is, ones in which attractions are important), close-packed configurations melt to the p3 phase, followed by the p6 phase, and finally a 2D gas phase. However, at high temperatures (that is, ones in which the attractions do not really play any role), we have found melting from the close-packed structure to a disordered fluid system. That is, the p6 and p3 phases are unstable with respect to these two phases. At intermediate temperatures, the p3 phase is observed on expansion of a close packed system, but this phase then melts directly to the disordered fluid, indicating that the temperature range of stability for the p3 phase is extended compared to that of the p6 phase.

## VII. PHASE DIAGRAM

The phase diagram, derived from combining the stable phases and coexistence densities obtained from the different simulation techniques at different temperatures, is drawn schematically in Fig. 5. In this section we briefly comment on the location of the phases.

At high temperatures, the fluid phase (A) and a close-packed solid (B), resembling a slightly distorted hard disc compact structure are observed. We find no evidence for a liquid-gas type transition, that is, one ending in a critical point, for this range of attractions. However, we have checked that such a transition exists when the range is sufficiently large ( $r_c \sim 0.5\sigma$ ) as predicted by theory,<sup>22</sup> although for this range the attractive potential is not localized and the model is clearly not a good model for annexin V. At lower temperatures a very low-density gas undergoes a transition to the p6 phase upon increasing the chemical potential. The low-density boundary of the p6 phase is an empty honeycomb lattice (C). On increasing the chemical potential–density–pressure, the empty cages are gradually filled by “adsorbed” trimers (D) until all the holes are filled (E). The system is driven into the p3 phase through a first-order transition. Even if the density range over which the p3 phase is stable is rather narrow, we can distinguish between an “untilted” (F) p3 and a “tilted” (G) p3\* phase. In the tilted variant, three vertices join at a bonding site slightly off center. The system responds to a density increase and tend to pack more efficiently by increasing the tilt, albeit with a slight energetic cost. The “chirality” of the bonding centers arises spontaneously during the simulation and is consistent throughout the sample. The critical temperature above which the p3 phase is no longer stable is found to be above that for the p6 phase.

We should point out that, whilst these phases can be observed for the simple model, they may not all be stable for real annexin V systems. For example, as already pointed out, if the particle shape is chiral, this may lead to a single, tilted p3 phase. It is also likely that the real systems cannot be forced to high enough density to observe the close packed structure; recall that we are only simulating the surface, and not the solution above the surface. In reality, if the protein solution density is so high as to force the surface density into this region, then it is unlikely that the surface can be thought of as an isolated entity. However, the predicted phase diagram does raise some interesting questions, such as do the p3 and p6 phases melt at different temperatures as found in the simulations, or do both phases disappear at the same temperature. Also, the simulations indicate that the p6 phase could be carefully “washed” of the captured trimers by decreasing the protein concentration in solution, to leave an empty honeycomb structure of reproducible dimensions which could be used for templating. As far as we are aware, this has not been investigated to date.

### VIII. CONCLUSIONS

The bulk thermodynamic properties of annexin V originate from a varied and complex combination of interactions. Nevertheless, a simple model based on the interactions between pairs of molecules is able to reproduce qualitatively the experimental observation of two crystalline phases (p6

and p3), and quantitatively the 15% density gap at the transition between these phases. The honeycomb network in the p6 phase can be mapped onto an ideal lattice gas problem, and the simple statistical mechanical theory reproduces the simulation data with no adjustable parameters. The phase diagram, derived by combining information from complementary simulation techniques, indicates that a low density gas phase and a high density close-packed solid phase should occur, although these may be inaccessible experimentally.

It is clear that, although the model described in this paper is relatively crude compared to the atomic detail model which could be constructed from the chemical structure of the molecules, such models should provide a useful test-bed for ideas concerning the mesoscopic assembly of biological systems, since they can tackle the large length scales precluded in an all atom description simulation.

### ACKNOWLEDGMENTS

The work of the FOM Institute is part of the research program of “Stichting Fundamenteel Onderzoek der Materie” (FOM) and is supported by NWO. M.G.N. acknowledges financial support from the “Marie Curie Fellowship” EU Contract No. ERBFMBICT982949.

- <sup>1</sup> See, for example, L. X. Yeu, J. B. Peng, M. A. Hediger, and D. E. Clapham, *Nature (London)* **410**, 705 (2001); L. W. Runnels, L. X. Yue, and D. E. Clapham, *Science* **291**, 1043 (2001).
- <sup>2</sup> W. M. Gelbart, A. Ben-Shaul, and Didier Roux, *Micelles, Membranes, Microemulsions, and Monolayers* (Springer-Verlag, New York, 1994).
- <sup>3</sup> P. Demange, D. Voges, J. Benz, S. Liemann, P. Gottig, R. Berendes, A. Burger, and R. Huber, *Trends Biochem. Sci.* **19**, 272 (1994).
- <sup>4</sup> O. G. Mouritsen, *Curr. Opin. Colloid Interface Sci.* **3**, 78 (1998).
- <sup>5</sup> M. G. Noro and D. Frenkel, *J. Chem. Phys.* **114**, 2477 (2001).
- <sup>6</sup> P. G. Dommersnes and J. B. Fournier, *Eur. Phys. J. B* **12**, 9 (1999).
- <sup>7</sup> W. M. Gelbart, R. P. Sear, J. R. Heath, and S. Chaney, *Faraday Discuss.* **122**, 299 (1999).
- <sup>8</sup> F. Carlsson, M. Malmsten, and P. Linse, *J. Phys. Chem. B* **105**, 12190 (2001).
- <sup>9</sup> E. E. Uzgiris and R. D. Kornberg, *Nature (London)* **301**, 125 (1983).
- <sup>10</sup> A. Brisson, A. Olofsson, P. Ringler, M. Schmutz, and S. Stoylova, *Biocell* **80**, 221 (1994).
- <sup>11</sup> I. Reviakine, W. Bergsma-Schutter, C. Mazeris-Dobut, N. Govorukhina, and A. Brisson, *J. Struct. Biol.* **131**, 234 (2000).
- <sup>12</sup> G. Mosser, C. Ravanat, J.-M. Freyssinet, and A. Brisson, *J. Mol. Biol.* **217**, 241 (1991).
- <sup>13</sup> I. Reviakine, W. Bergsma-Schutter, A. N. Morozov, and A. Brisson, *Langmuir* **17**, 1680 (2001).
- <sup>14</sup> M. G. Noro, M. A. Bates, A. Brisson, and D. Frenkel, *Langmuir* (in press).
- <sup>15</sup> A. Brisson, W. Bergsma-Schutter, F. Oling, O. Lambert, and I. Reviakine, *J. Cryst. Growth* **196**, 456 (1999).
- <sup>16</sup> A. Brisson (personal communications).
- <sup>17</sup> D. Frenkel and B. Smit, *Understanding Molecular Simulations* (Academic, New York, 1996).
- <sup>18</sup> T. Hill, *An Introduction to Statistical Thermodynamics* (Dover, New York, 1986).
- <sup>19</sup> M. P. Allen and D. J. Tildesley, *Computer Simulation of Liquids* (Oxford University Press, Oxford, 1987).
- <sup>20</sup> For a review on the cluster move, see K. Binder, *Applications of the Monte Carlo Method in Statistical Physics* (Springer, Berlin, 1984).
- <sup>21</sup> A. D. Mackie, A. Z. Panagiotopoulos, D. Frenkel, and S. K. Kumar, *Eur. Phys. Lett.* **27**, 549 (1994).
- <sup>22</sup> M. G. Noro and D. Frenkel, *J. Chem. Phys.* **113**, 2941 (2000).